Japanese Journal of Applied Physics **57**, 068001 (2018)
https://doi.org/10.7567/JJAP.57.068001

BRIEF NOTE

Platinum-free, carbon-based materials as efficient counter electrodes for dye-sensitized solar cells

Hendri Widiyandari[1]*, Adi Prasetio[2], Agus Purwanto[3], Agus Subagio[2], and Rachmat Hidayat[4]

[1]*Department of Physics, Faculty of Mathematics and Natural Science, Sebelas Maret University, Surakarta 57126, Indonesia*
[2]*Department of Physics, Faculty of Science and Mathematics, Diponegoro University, Semarang 50275, Indonesia*
[3]*Department of Chemical Engineering, Faculty of Engineering, Sebelas Maret University, Surakarta 57126, Indonesia*
[4]*Department of Physics, Institut Teknologi Bandung, Bandung 40132, Indonesia*

*E-mail: hendriwidiyandari@staff.uns.ac.id

Received February 2, 2018; accepted March 23, 2018; published online May 22, 2018

The electrocatalytic potential of carbon materials makes them the most viable candidate to replace Pt as a counter electrode (CE) in dye-sensitized solar cells (DSSCs). In this research, we report our study using graphite, CNT/graphite composite, CNT, and Pt-based CEs in DSSCs. The electrochemical impedance spectroscopy (EIS) measurement showed that the CNT-based CE (CNT-CE) has the lowest charge transport resistance (R_{ct}) compared with graphite and the CNT/graphite composite. The photovoltaic performance measurement showed that the CNT-CE resulted in a short-circuit photocurrent density (J_{sc}) of 3.59 mA·cm^{-2} whereas the Pt-based CE (Pt-CE) resulted in a J_{sc} of 2.76 mA·cm^{-2}.

Dye-sensitized solar cells (DSSCs) have attracted attention because of their high conversion efficiency, low-cost, and easy fabrication.[1–3] Basically, a DSSC consists of transparent conducting oxide (TCO) glass coated with a wide-band-gap semiconductor, a Ru-based sensitizer, an electrolyte containing an I^-/I_3^- redox couple, and a counter electrode (CE).[4] Over the past two decades, the seemingly constant development of DSSC technology has markedly improved the photovoltaic performance. One of the most important developments has resulted in an increase in the performance of CEs. The regeneration process has been accelerated from I_3^- to I^-, and the electron transfer activity has been increased from an external load to an electrolyte solution.[5,6] Platinum (Pt) is the most widely used CE material owing to its excellent electric conductivity and electrocatalytic activity.[7] Pt, however, is an expensive noble metal with high processing temperature and is prone to corrosion from electrolytes, which necessitates its replacement.[8,9]

Carbon materials are the most promising materials to replace Pt because of their high conductivity, high electrocatalytic activity, and corrosion resistance.[10–13] Graphite is an inexpensive carbon material with excellent intrinsic conductivity. However, graphite has a very poor catalytic activity when used as a CE material for DSSC application.[14] There are many attempts to improve the photovoltaic properties of carbon-CE-based DSSCs. Li et al. reported solely a natural graphite material with different structures (nanofiber, nanosheet, and nanoball).[15] Veerappan et al. used sub-micrometer-sized graphite as a conducting film and a CE simultaneously.[16] Carbon nanotubes (CNTs) are allotropes of carbon with a cylindrical nanostructure, which are classified into two types, i.e., single-walled CNTs and multiwalled CNTs. The conductivity and corrosion resistance of the CNTs, however, have continued to fascinate researchers who continue to search for what gives these materials their unique properties. In several attempts, CNTs have improved the photovoltaic performance of DSSCs.[17–19] The specific surface area, stability in general electrolytes including the redox couple in DSSCs, and the electrocatalytic activity of the catalyst play important roles in improving the working capability of the counter electrode.

The electrocatalytic activity of the catalyst as the CE for DSSC application is measured by electrochemical impedance spectroscopy (EIS). Chiba et al. reported the internal resistance of DSSCs measured by EIS to investigate DSSC mechanisms as well as propose an equivalent circuit for modeling DSSCs based on the results of EIS analysis.[3] On the basis of the modeling, the internal resistance of DSSCs consists of three resistance elements, i.e., the sheet resistance of the TCO, the resistance of ionic diffusion in the electrolyte, and the resistance at the interface between the counter electrode and the electrolyte. The internal resistance affects *FF* and J_{sc}, that is, a lower internal resistance in a device increases *FF* and J_{sc}.

In this paper, we present our investigation of the relationship between the charge transport resistance at the CE/electrolyte interface and photovoltaic parameters, such as short-circuit current density and open-circuit voltage that affects the conversion efficiency of DSSCs using carbon-based CEs consisting of graphite, CNT/graphite composite, and CNTs. Commercial Pt was also used in this study for comparison.

In this experiment, CNTs were synthesized by spray pyrolysis. The precursor of CNTs was prepared by mixing 0.6 g of ferrocene (Merck) in 10 mL of benzene (Merck). The precursor solution was dispersed into fine droplets using a syringe pump. The droplets flowed into the electrical tubular furnace and heated at 900 °C. The collected CNTs were refluxed using 65% HNO_3 for 4 h at 100 °C. The amounts of CNTs and HNO_3 solution are 0.1 g and 50 mL, respectively. CNT powder was obtained by filtering and drying the refluxed CNTs at 120 °C overnight. Carbon-based CEs were prepared from CNTs, graphite (Merck), and CNT–graphite composite with 1 : 1 of %wt. The preparation of carbon-based CEs was carried out in two steps: preparing the carbon paste and then coating the substrate with the paste by the doctor-blade method. The carbon paste was prepared by mixing 0.2 g of ethyl cellulose (Sigma Aldrich) in 2 ml of ethanol with stirring for 5 min, followed by mixing 0.8 g of terpineol (Sigma Aldrich) in the solution used as the binder. The carbon powder was dispersed in the binder with stirring for 5 min. The resulting carbon paste was deposited on a 1 cm^2 area of a fluorine-doped tin oxide (FTO) glass substrate (15 Ω/□, Dyesol) via the doctor-blade method, followed by drying at 80 °C for 5 min and annealing at 450 °C for 1 h. The thickness of the carbon film depends on that of scotch tape. DSSCs were assembled firstly by preparing a TiO_2-based

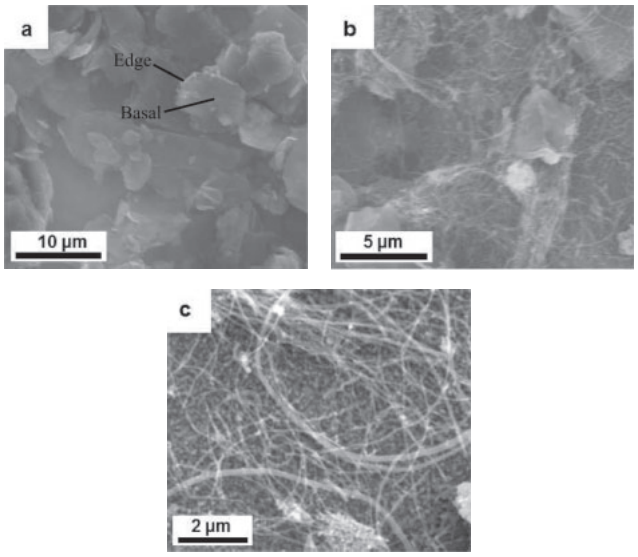

Fig. 1. SEM images of (a) graphite (b) CNT/graphite composite, and (c) CNTs deposited on FTO substrates.

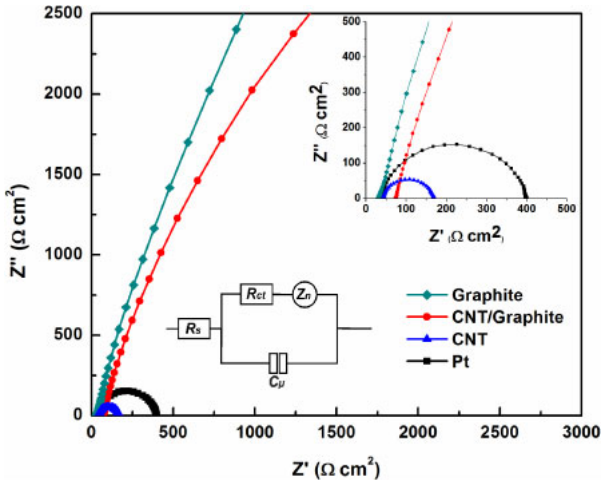

Fig. 2. (Color online) Nyquist plot of the symmetrical cell using graphite, CNT/graphite composite, CNTs, and Pt electrodes clipping the I^-/I_3^- electrolyte. The equivalent circuit model and zoom out of Nyquist plot are given in the inset.

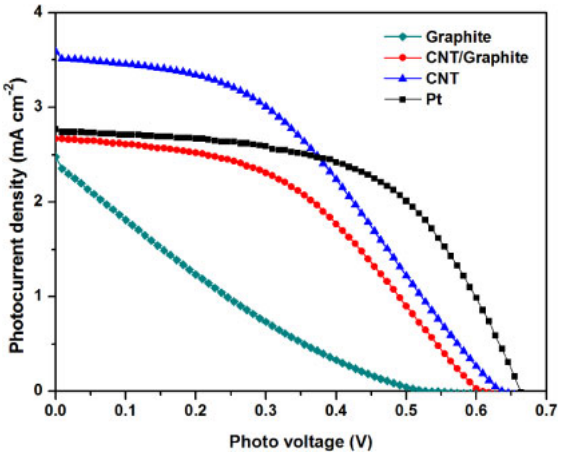

Fig. 3. (Color online) *J*–*V* curves of DSSCs using carbon-based CEs.

photoanode. TiO_2 nanoparticle paste (Dyesol, 20 nm) was deposited on the FTO glass substrate by the doctor-blade method and annealed at 500 °C for 45 min. The photoanode was then immersed in 0.3 mM Ru dye (Dyesol N719) solution at room temperature for 24 h. Finally, both the photoanode and a CE were assembled into a sandwiched structure with a sealant as a spacer between the two electrodes. An electrolyte solution containing an I^-/I_3^- redox couple (Dyesol HSE) was injected into the gap between the two electrodes. The surface morphology of the carbon-based CE was observed by scanning electron microscopy (SEM; JEOL JSM-6360 LA). EIS was carried out in the dark using an electrochemical instrument (Gamry Instrument Reference 3000) in a frequency range of 0.01 Hz to 65 kHz and the applied bias voltage was set at 10 mV. The photovoltaic properties of the assembled DSSCs were measured using an AM 1.5 G solar simulator with a light intensity of 100 mW·cm^{-2} (Abet Technology Sun 2000 solar simulators) equipped with a digital sourcemeter (Keithley 2602A).

Figure 1 shows SEM images of the carbon-based CEs. Figure 1(a) shows how graphite creates an abundant basal plane with fewer edges because it is composed of large particles. The CNTs were randomly distributed among the graphite particle [Fig. 1(b)], and tended to cover both the basal plane and the empty areas, which increased the surface area. Figure 1(c) shows how the tubular shapes of the CNTs created a random orientation that allowed them to weave together.

EIS is the most common technique used to determine the internal resistance of DSSCs with different interfaces.[20] In this research, we only determined the first semicircle that corresponds to the charge transport resistance (R_{ct}) at the CE/electrolyte interface. Figure 2 shows a Nyquist plot with an equivalent circuit diagram of the carbon-CEs. The R_{ct} values of graphite, the CNT/graphite composite, CNTs, and Pt were 555.1, 384.3, 239.9, and 104.8 Ω·cm^2, respectively. The lowest R_{ct} in the CNT-CEs indicates that the highest electrocatalytic ability was recorded using the electrodes through I_3^- reduction.

The conversion efficiency (η) of solar cells can be expressed as

$$\eta = FF \times J_{sc} \times V_{oc}/P_{in}, \quad (1)$$

where FF, J_{sc}, V_{oc}, and P_{in} are the fill factor, short-circuit current density, open-circuit voltage, and incident light power (100 mW·cm^{-2}), respectively. FF is determined by

$$FF = \frac{V_{max}J_{max}}{V_{oc}J_{sc}}, \quad (2)$$

where V_{max} and I_{max} represent the voltage and photocurrent at the maximum output power point, respectively. Equation (1) suggests that it should be necessary to improve these three parameters in order to increase the conversion efficiency. Figure 3 shows the photocurrent density–voltage (*J*–*V*) curves of the DSSCs. The photovoltaic performance and electrocatalytic parameters of the DSSCs are listed in Table I. The J_{sc} values of graphite, the CNT/graphite composite, CNTs, and Pt were 2.48, 2.68, 3.59, and 2.78 mA·cm^{-2}, respectively. The one-dimensional structure of CNTs [Fig. 1(b)] gave them the highest J_{sc} and the lowest R_{ct} because of good electron transfer kinetics. Although the CNTs had a lower V_{oc} and FF, they nonetheless had the lowest R_{ct}, which indicated that the I_3^- reduction showed the highest conductivity and electrocatalytic ability.[21] By comparison, graphite with a large basal plane showed the lowest J_{sc} and

Table I. Photovoltaic performance of the DSSCs using various CEs and the electrocatalytic parameters of the CEs.

	V_{max} (V)	J_{max} (mA·cm^{-2})	V_{oc} (V)	J_{sc} (mA·cm^{-2})	R_{ct} (Ω·cm^2)	FF	η (%)
Graphite	0.21	1.20	0.53	2.48	555.1	0.19	0.25
CNT/graphite	0.36	2.03	0.61	2.68	384.3	0.45	0.72
CNT	0.34	2.71	0.64	3.59	104.8	0.40	0.94
Pt	0.46	2.16	0.66	2.78	239.0	0.54	1.01

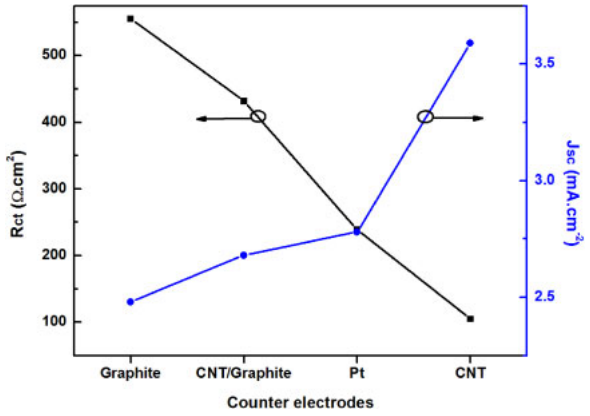

Fig. 4. (Color online) Relationship between charge transfer resistance (R_{ct}) and short-circuit photocurrent density (J_{sc}).

highest R_{ct} owing to its slow electron transfer kinetics and a small number of catalytic sites.[16] The Pt and CNT/graphite composite showed similar J_{sc} values. The high J_{sc} of the CNT/graphite composite was probably caused by its large surface area, wherein the empty areas in the graphite were filled with CNTs. Thus, a low R_{ct} significantly improves the electrocatalytic activity and electrical conductivity at the CE/electrolyte interface. This condition directly increases the density of transfer electrons, as represented by J_{sc}. An increase in J_{sc} is inversely related to R_{ct}, as shown in Fig. 4. Thus, from Eq. (1), it is clear that, to improve the conversion efficiency, J_{sc} should be increased.

In conclusion, we fabricated CEs for use in DSSCs by depositing carbon materials onto FTO glass substrates via the doctor-blade method. The resultant decrease in charge transfer resistance was related to the enhancement of the electron transfer activity at the CE/electrolyte surface. In this study, CNT CEs exhibited the highest J_{sc} and lowest R_{ct}, and proved to be the optimal carbon material choice to replace Pt-coated CEs.

Acknowledgments This research was financially supported by the Indonesia Toray Science Foundation (ITSF). The authors also greatly thank Muhammad Hilmy Alfaruqi (Chonnam National University) for valuable discussion.

1) B. O'Regan and M. Grätzel, Nature **353**, 737 (1991).
2) K. Nazeeruddin, E. Baranoff, and M. Grätzel, Sol. Energy **85**, 1172 (2011).
3) Y. Chiba, A. Islam, Y. Watanabe, R. Komiya, N. Koide, and L. Han, Jpn. J. Appl. Phys. **45**, L638 (2006).
4) J. Feng, Y. Jiao, W. Ma, M. K. Nazeeruddin, M. Grätzel, and S. Meng, J. Phys. Chem. C **117**, 3772 (2013).
5) M. Ye, X. Wen, M. Wang, J. Iocozzia, N. Zhang, C. Lin, and Z. Lin, Mater. Today **18**, 155 (2015).
6) S. Thomas, T. G. Deepak, G. S. Anjusree, T. Arun, S. V. Nair, and S. Nair, J. Mater. Chem. A **2**, 4474 (2014).
7) Y. L. Lee, C. L. Chen, L. W. Chong, C. H. Chen, Y. F. Liu, and C. F. Chi, Electrochem. Commun. **12**, 1662 (2010).
8) S. Yun, A. Hagfeldt, and T. Ma, Adv. Mater. **26**, 6210 (2014).
9) Q. W. Jiang, G. R. Li, and X. P. Gao, Chem. Commun. **44**, 6720 (2009).
10) H. Kim, H. Choi, S. Hwang, Y. Kim, and M. Jeon, Nanoscale Res. Lett. **7**, 53 (2012).
11) W. J. Lee, E. Ramasamy, D. Y. Lee, and J. S. Song, Sol. Energy Mater. Sol. Cells **92**, 814 (2008).
12) T. Adachi and H. Hoshi, Mater. Lett. **94**, 15 (2013).
13) C. S. Chen and C. K. Hsieh, Jpn. J. Appl. Phys. **53**, 11RE02 (2014).
14) S. Gagliardi, L. Giorgi, R. Giorgi, N. Lisi, T. Dikonimos Makris, E. Salernitano, and A. Rufoloni, Superlattices Microstruct. **46**, 205 (2009).
15) Y. Y. Li, C. T. Li, M. H. Yeh, K. C. Huang, P. W. Chen, R. Vittal, and K. C. Ho, Electrochim. Acta **179**, 211 (2015).
16) G. Veerappan, K. Bojan, and S. W. Rhee, ACS Appl. Mater. Interfaces **3**, 857 (2011).
17) G. Yue, J. Zhang, J. Liu, X. Lu, Z. Hu, and Y. Zhu, J. Mater. Sci.: Mater. Electron. **27**, 4736 (2016).
18) R. A. Sayer, S. L. Hodson, and T. S. Fisher, J. Sol. Energy Eng. **132**, 021007 (2010).
19) F. M. Al-Marzouki, S. Abdalla, and S. Al-Ameer, Adv. Mater. Sci. Eng. **2016**, 1 (2016).
20) K. M. Lee, C. Y. Hsu, P. Y. Chen, M. Ikegami, T. Miyasaka, and K. C. Ho, Phys. Chem. Chem. Phys. **11**, 3375 (2009).
21) P. L. McEuen, M. Bockrath, D. H. Cobden, and J. G. Lu, Microelectron. Eng. **47**, 417 (1999).